Study of Conservation on Implicit Techniques for Unstructured Finite Volume Navier-Stokes Solvers

Carlos Junqueira-Junior, junior.hmg@gmail.com
Instituto Tecnológico de Aeronáutica – ITA, São José dos Campos, SP, Brazil

Leonardo Costa Scalabrin, leonardo.scalabrin@embraer.com.br
EMBRAER S.A., São José dos Campos, SP, Brazil

Edson Basso, edsonbss@gmail.com
João Luiz F. Azevedo, joaoluiz.azevedo@gmail.com
Instituto de Aeronáutica e Espaço – IAE, São José dos Campos, SP, Brazil

Abstract. *The work is an study of conservation on linearization techniques of time-marching schemes for unstructured finite volume Reynolds-averaged Navier-Stokes formulation. The solver used in this work calculates the numerical flux applying an upwind discretization based on the flux vector splitting scheme. This numerical treatment results in a very large sparse linear system. The direct solution of this full implicit linear system is very expensive and, in most cases, impractical. There are several numerical approaches which are commonly used by the scientific community to treat sparse linear systems, and the point-implicit integration was selected in the present case. However, numerical approaches to solve implicit linear systems can be non-conservative in time, even for formulations which are conservative by construction, as the finite volume techniques. Moreover, there are physical problems which strongly demand conservative schemes in order to achieve the correct numerical solution. The work presents results of numerical simulations to evaluate the conservation of implicit and explicit time-marching methods and discusses numerical requirements that can help avoiding such non-conservation issues.*

Keywords: *Computational Fluid Dynamics, Time Maching Methods, Flux Vector Splitting Scheme, Conservative Discretization*

1. NOMENCLATURE

English Characters

A	Jacobian matrix of the numerical flux
F	Numerical flux vector
n	Normal vector
nf	Number of faces of a given volume
Q	Conserved variable vector
S	Area
t	Time

Subscripts

cl	Cell on the left side of the face
cr	Cell on the right side of the face
k	Index of the cell face

Superscripts

n	Index of iteration in time
p	Index of iteration for the point-implicit time integration

2. INTRODUCTION

This work discusses issues associated with the coupling of implicit integration methods, for unstructured finite volume formulations, with the spatial discretization based on flux vector splitting schemes. The material discussed in this work is an extension of the work of Barth (1987). The original paper discussed approximate local time linearizations of nonlinear terms for the finite difference formulation using TVD (Harten, 1983) and upwind algorithms. Here, the time conservation of the point-implicit integration for unstructured meshes is analyzed and discussed. Finite volume formulations have the tremendously important property of being conservative by construction. However, some time integration approaches

may present numerical issues that can destroy this property, at least for unsteady applications or during the process of converging to a steady state. This shortcoming was noted by the research group during the execution of closed system simulations. There was heat generation and non-conservation of the mass in the interior domain. Results of simulations using explicit and implicit integration are presented in this work to better understand the non conservation issue of time-marching methods. An analysis of the problem is also performed by a detailed study of the backward Euler linearization.

3. NUMERICAL FORMULATION

The numerical formulation applied in this work is briefly presented in this section. All the study is performed using the Reynolds-averaged Navier-Stokes equations, which is written here in the context of a cell-centered finite-volume formulation as

$$\frac{\partial Q_i}{\partial t} = -\frac{1}{V_i}\sum_{k=1}^{nf} \overrightarrow{F_k}\cdot\overrightarrow{n_k}\,S_k\ . \tag{1}$$

in which, Q, is vector of conservative properties, V, is the volume of the cell, F, is the numerical flux through the faces of the cell, $\overrightarrow{n}$, is the outward normal face vector, and S, is the surface of the face. The subscripts, k and i, indicate the face index and cells index, respectively and the superscrip nf indicates the number of faces of the i-th cell.

3.1 Inviscid flux calculation

The inviscid fluxes are calculated using a method based on a classical flux vector splitting formulation, the Steger-Warming scheme (Steger and Warming, 1981). This method is an upwind scheme that uses the homogeneous property of the inviscid flux vectors to write

$$\overrightarrow{F_k}\cdot\overrightarrow{n_k} \;=\; F_n \;=\; \frac{\partial F_n}{\partial Q}\,Q \;=\; A\,Q\ , \tag{2}$$

where F_n is the normal flux at the k-th face, and A is the Jacobian matrix of the inviscid flux that can be diagonalized by the matrices of its eigenvectors from the left and from the right, L and R

$$A \;=\; R\,\Lambda\,L\ , \tag{3}$$

and Λ is the diagonal matrix of the eigenvalues of the Jacobian matrix. The A matrix can be split into positive and negative parts as

$$A^{+} \;=\; R\,\Lambda^{+}\,L \quad \text{and} \quad A^{-} \;=\; R\,\Lambda^{-}\,L\ . \tag{4}$$

The splitting separates the flux into two parts, the downstream and the upstream flux, in relation to the face orientation as

$$\overrightarrow{F}\cdot\overrightarrow{n} \;=\; F_n^{+} \,+\, F_n^{-} \;=\; \left(A_{cl}^{+}\,Q_{cl} \,+\, A_{cr}^{-}\,Q_{cr}\right)\ , \tag{5}$$

where the cl and cr subscripts are the cells on the left and right sides of the face. The split eigenvalues of the Jacobian matrix are given by

$$\lambda^{\pm} = \frac{1}{2}\left(\lambda \,\pm\, |\lambda|\right)\ . \tag{6}$$

Numerical studies indicate that this flux vector splitting is too dissipative and it can deteriorate the boundary layer profiles (MacCormack and Candler, 1989; Junqueira-Junior *et al.*, 2011; Junqueira-Junior, 2012; Scalabrin, 2007). Therefore, a pressure switch is used to smoothly shift the Steger-Warming scheme into a centered one. Hence, the artificial dissipation

is controlled and the numerical stabillity is maintained. The modified formulation can be written as

$$\overrightarrow{F_k} \cdot \overrightarrow{n_k} \;=\; F_k^+ \;+\; F_k^- \;=\; \left(A_{k^+}^+ \, Q_{k^+} \;+\; A_{k^-}^- \, Q_{k^-}\right) \tag{7}$$

in which

$$Q_{k^+} \;=\; (1-w)\, Q_{cl} \;+\; w\, Q_{cr} \qquad \text{and} \qquad Q_{k^-} \;=\; (1-w)\, Q_{cr} \;+\; w\, Q_{cl} \;. \tag{8}$$

The switch, w, is given by

$$w \;=\; \frac{1}{2}\,\frac{1}{(\alpha \nabla p)^2 + 1} \qquad \text{and} \qquad \nabla p \;=\; \frac{|p_{cl} - p_{cr}|}{\min(p_{cl}, p_{cr})} \;. \tag{9}$$

Therefore, for small ∇p, $w = (1-w) = 0.5$, and the code runs with a centered scheme. For large values of ∇p, $w = 0$ and $(1-w) = 1$, and the code runs with the standard Steger-Warming scheme. For Eq. (9), the literature suggests using $\alpha = 6$, but some problems may require larger values (Scalabrin, 2007).

3.2 Viscous flux calculation

The viscous terms are based on derivative of properties on the faces. To build the derivative terms, two volumes are created over the face where the derivative is being calculated. At the center of each new volume, the derivative is calculated using the Green-Gauss theorem. This computation is used to find the derivative at the desired face. The work of Scalabrin (2007) and of Junqueira-Junior (2012) provide further details on the viscous flux computations.

3.3 Time integration

In the present work, two time-marching methods are applied, the explicit second-order Runge-Kutta method (Lomax *et al.*, 2001) and the point implicit scheme.

3.3.1 Second-order Runge-Kutta method

The second-order Runge-Kutta integration method used in this work is given by

$$\text{Predictor step:} \quad \begin{cases} \Delta Q_i^n \;=\; -\dfrac{\Delta t}{V_i}\left[\displaystyle\sum_{k=1}^{nf} \overrightarrow{F_k} \cdot \overrightarrow{n_k}\, S_k\right]^n \;=\; R_i^n \\ Q_i^{\overline{n+1}} \;=\; Q_i^n \;+\; \Delta Q_i^n \end{cases}$$

$$\text{Corrector step:} \quad \begin{cases} \Delta Q_i^{\overline{n+1}} \;=\; -\dfrac{\Delta t}{V_i}\left[\displaystyle\sum_{k=1}^{nf} \overrightarrow{F_k} \cdot \overrightarrow{n_k}\, S_k\right]^{\overline{n+1}} \;=\; R_i^{\overline{n+1}} \\ Q_i^{n+1} \;=\; \dfrac{1}{2}\left(Q_i^n \;+\; Q_i^{\overline{n+1}} \;+\; \Delta Q_i^{\overline{n+1}}\right) \end{cases} \tag{10}$$

in which R_i is the residue of the i-th cell.

3.3.2 Point implicit integration

The implicit integration method applied in this work is based on the backward Euler method, which can be written for the present case as

$$\Delta Q_i^n \;=\; -\,\frac{\Delta t}{V_i}\left[\sum_{k=1}^{nf} \overrightarrow{F_k} \cdot \overrightarrow{n_k}\, S_k\right]^{n+1} \;=\; R_i^{n+1} \;. \tag{11}$$

One can linearize the residue at time $n+1$ as a function of properties at time n and apply the spatial discretization and the face-based notation in order to write

$$\left[\frac{V_{cl}}{\Delta t} + \sum_{k=1}^{nf} A_{k+}^{+} S_k\right] \Delta Q_{cl}^{n} + \sum_{k=1}^{nf} A_{k-}^{-} S_k \Delta Q_{cr,k}^{n} = R_{cl}^{n} . \tag{12}$$

In a simpler form, one can write

$$[M] \Delta Q_{cl}^{n} + \frac{V_{cl}}{\Delta t} [I] \Delta Q_{cl}^{n} = R_{cl}^{n} . \tag{13}$$

The implicit integration of unstructured meshes is very expensive and, in most cases, impractical, because it generates very large sparse linear systems. An approximate method, the point-implicit integration, is applied in the present work (Scalabrin, 2007; Junqueira-Junior, 2012). For this time-marching method, the $[M]$ matrix, presented in Eq. (13), is split into a diagonal matrix, $[M]_d$, and an off-diagonal matrix, $[M]_{od}$, as

$$[M] = [M_d] + [M_{od}] . \tag{14}$$

Then, the linear system is written as

$$[M_d] \Delta Q_{cl}^{p} + \frac{V_{cl}}{\Delta t} [I] \Delta Q_{cl}^{p} = R_{cl}^{n} - [M_{od}] \Delta Q_{cl}^{p-1} . \tag{15}$$

The point-implicit method performs sub-iterations, in p, until a predefined number of sub-iterations or until the convergence of ΔQ_{cl}. The sub-iterations are started assuming that $\Delta Q_{cl}^{0} = 0$.

4. CONSERVATION ANALYSIS OF IMPLICIT METHODS

4.1 General conservation analysis

After this brief review, the backward Euler time marching method, given by Eq. (13), is applied on a generic grid, which is a representative 2-D finite volume mesh using nine quad-cells, as illustrated in Fig. 1, in order to present the conservative issues of such linearization. The $[M]$ matrix, for the mesh used here, is represented by

$$[M] = \begin{bmatrix}
\sum A_1^+ & A_{1,2}^- & & A_{1,4}^- & & & & & \\
A_{2,1}^- & \sum A_2^+ & A_{3,3}^- & & A_{3,5}^- & & & & \\
 & A_{3,2}^- & \sum A_3^+ & & A_{3,5}^- & & & & \\
A_{4,1}^- & & & \sum A_4^+ & A_{4,5}^- & & A_{4,8}^- & & \\
 & A_{5,2}^- & & & \sum A_5^+ & A_{5,6}^- & & A_{5,8}^- & \\
 & & A_{6,3}^- & & A_{6,5}^- & \sum A_6^+ & & & A_{6,9}^- \\
 & & & A_{7,4}^- & & & \sum A_7^+ & A_{7,8}^- & \\
 & & & & A_{8,5}^- & & A_{8,7}^- & \sum A_8^+ & A_{8,9}^- \\
 & & & & & A_{9,6}^- & & A_{9,8}^- & \sum A_9^+
\end{bmatrix} . \tag{16}$$

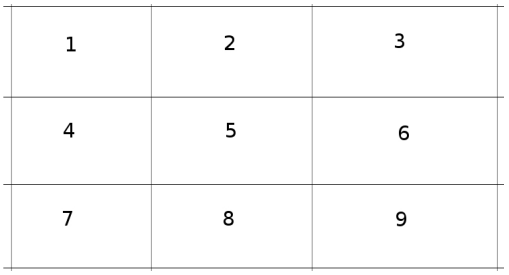

Figure 1. Representative 2-D finite volume mesh.

The formulation can be considered conservative when the sum of $V_i \Delta Q_i^n$ terms, for all cells, yields zero, *i.e.*,

$$\sum \left[V_i \, \Delta Q_i^n \right] \, = \, 0 \, , \quad \text{or yet} \quad \sum \left[V_i \, Q_i^n \right] \, = \, \sum \left[V_i \, Q_i^{n+1} \right] \, . \tag{17}$$

Solving the linear system for the converged solution, which means that $R_i^n = 0$, one obtains

$$\left[\frac{V_1}{\Delta t} + \sum A_1^+ + A_{2,1}^- + A_{4,1}^- \right] \, \Delta Q_1 + \left[\frac{V_2}{\Delta t} + A_{1,2}^- + \sum A_2^+ + A_{3,2}^- + A_{5,2}^- \right] \, \Delta Q_2 + ... = 0 \, . \tag{18}$$

It is possible to simplify this equation in order to write

$$\left[\frac{V_1}{\Delta t} + [C_1] \right] \, \Delta Q_1 + \left[\frac{V_2}{\Delta t} + [C_2] \right] \, \Delta Q_2 + ... = 0 \, , \tag{19}$$

where the $[C_i]$ matrix is the sum of the inviscid and viscous Jacobian matrices in each column of the $[M]$ matrix. Comparing Eqs. (17) and (19), one can easily state that, to preserve the conservative property of the finite volume formulation, the $[C_i]$ matrices should be zero and Δt should be the same for all the cells in the domain, *i.e.*,

$$\left[\frac{V_1}{\Delta t} \right] \, \Delta Q_1 + \left[\frac{V_2}{\Delta t} \right] \, \Delta Q_2 + ... \, = \, \frac{1}{\Delta t} \sum \left[V_i \, \Delta Q_i^n \right] \, = \, 0 \, . \tag{20}$$

4.2 Point implicit conservation analysis

If one solves the linear system for the same mesh presented in Fig. 1 using the point-implicit integration, after a converged solution is obtained, *i.e.*, $R_i^n = 0$, one could finally write

$$\begin{aligned} & \left\{ \left[\frac{V_1}{\Delta t} \, + \sum A_1^+ \right] \, \Delta Q_1^p \, + \, \left[A_{2,1}^- \, + \, A_{4,1}^- \right] \, \Delta Q_1^{p-1} \right\} \\ + \quad & \left\{ \left[\frac{V_2}{\Delta t} \, + \sum A_2^+ \right] \, \Delta Q_2^p \, + \, \left[A_{1,2}^- \, + \, A_{3,2}^- \, + \, A_{5,2}^- \right] \, \Delta Q_2^{p-1} \right\} \, + \, ... \, = \, 0 \, . \end{aligned} \tag{21}$$

One can state that, as long the sub-iterations of the point implicit method have not achieved the convergence for ΔQ_i^p and/or Δt is not the same for all the cells in the domain, it is not possible to find a general relation for any ΔQ_i^p and ΔQ_i^{p-1} such that $\sum [V_i \Delta Q_i^n] = 0$. Therefore, the conservation property for the point-implicit integration can be achieved only if the $[C_i]$ matrices are zero, the solution of ΔQ_i^p for the sub-iterations in p is converged, and Δt is constant over the entire mesh.

However, achieving convergence of the point-implicit sub-iterations can be as expensive as performing the fully implicit integration. Hence, all practical numerical solvers perform a limited number of sub-iterations. The authors, usually, perform up to 10 sub-iteration in p for the point-implicit integration and, then, move on to the next time step. Typically, this is not enough to achieve convergence for ΔQ_i^p, as discussed the forthcoming section of the paper.

5. RESULTS AND DISCUSSION

Results for the so-called "rigid body simulation" problem are presented in this section in order to expose the effects of the time-marching scheme on the mass conservation. The rigid body problem consists of the simulation of the flow contained between two concentric cylinders, in which both walls rotate at the same angular velocity. Therefore, after convergence, the fluid in the domain is rotating at the same angular velocity as if it were a rigid body. Here, the problem is addressed as a 2-D flow. The present work performed simulations using the point-implicit and the Runge-Kutta time marching methods. An analysis of the use of a constant CFL number on all mesh cells is also presented here, in comparison to the use of a constant Δt throughout the mesh.

The two dimensional geometry and the detailed 360,000 cell mesh, used in the simulations, are presented in Fig. 2.

The external and internal cylinders are rotating walls with fixed angular velocity, ω, and fixed temperature, T_0. Air with

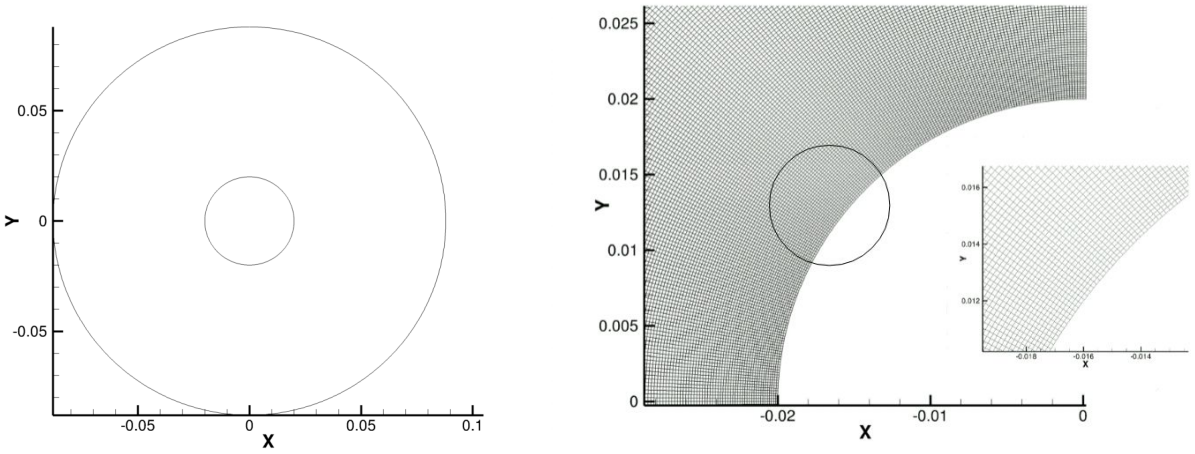

Figure 2. Rigid body geometry and mesh detail.

zero velocity and T_0 temperature are considered as initial conditions. All simulations are conducted with the same initial and boundary conditions. Each simulation is performed using a different time marching method, as presented in Table 1.

Table 1. Definition of the test case configurations for the numerical simulations.

Case	Time marching scheme	Constant Δt or CFL
1	Point implicit	Constant CFL
2	Point implicit	Constant Δt
3	Runge-Kutta	Constant CFL
4	Runge-Kutta	Constant Δt

Figure 3 presents the total amount of mass (per unit of length in the cylinder axial direction) inside the computational domain, as a function of the iteration number, for the rigid body simulations. It is clear from the figure that the point implicit time marching method can significantly deteriorate the important conservative property of the finite volume formulation. Moreover, both simulations with the point-implicit time-marching scheme presented exactly the same non-conservative behavior. Moreover, for the point-implicit time integration test cases, *i.e.*, test cases 1 and 2, or cases shown in Figs. 3 (a) and (b), there is almost no influence of the selection of constant CFL or of constant Δt in the time march. In other words, one could state that, for these test cases, the non-conservation effects of using a constant CFL number are far less significant than the effects of using the point implicit integration. Furthermore, it is correct to state that both simulations diverged after some time (not shown in Fig. 3).

In contrast to that behavior, simulations performed using the explicit Runge-Kutta scheme and a constant time step throughout the domain perfectly conserve the mass in the computational domain, as one would expect from a finite volume code. The results for this test case (case 4) are shown in Fig. 3 (d). On the other hand, results in Fig. 3 (c) indicate that, even with an explicit scheme, there is no mass conservation if a variable time step, or constant CFL number, is used in the time integration. This is a serious problem since most convergence acceleration procedures typically employed in aerospace CFD codes are based on the use of implicit integration or of variable time stepping, or both. The present results are clearly demonstrating that, for such cases, there is no mass conservation during the transient process of converging to a steady state solution.

Moreover, all results presented in Fig. 3 reinforce the previous analysis performed in this work. To assure the conservative property of a time marching method, the $[C_i]$ matrix shoud be zero. This is automatically enforced by the explicit

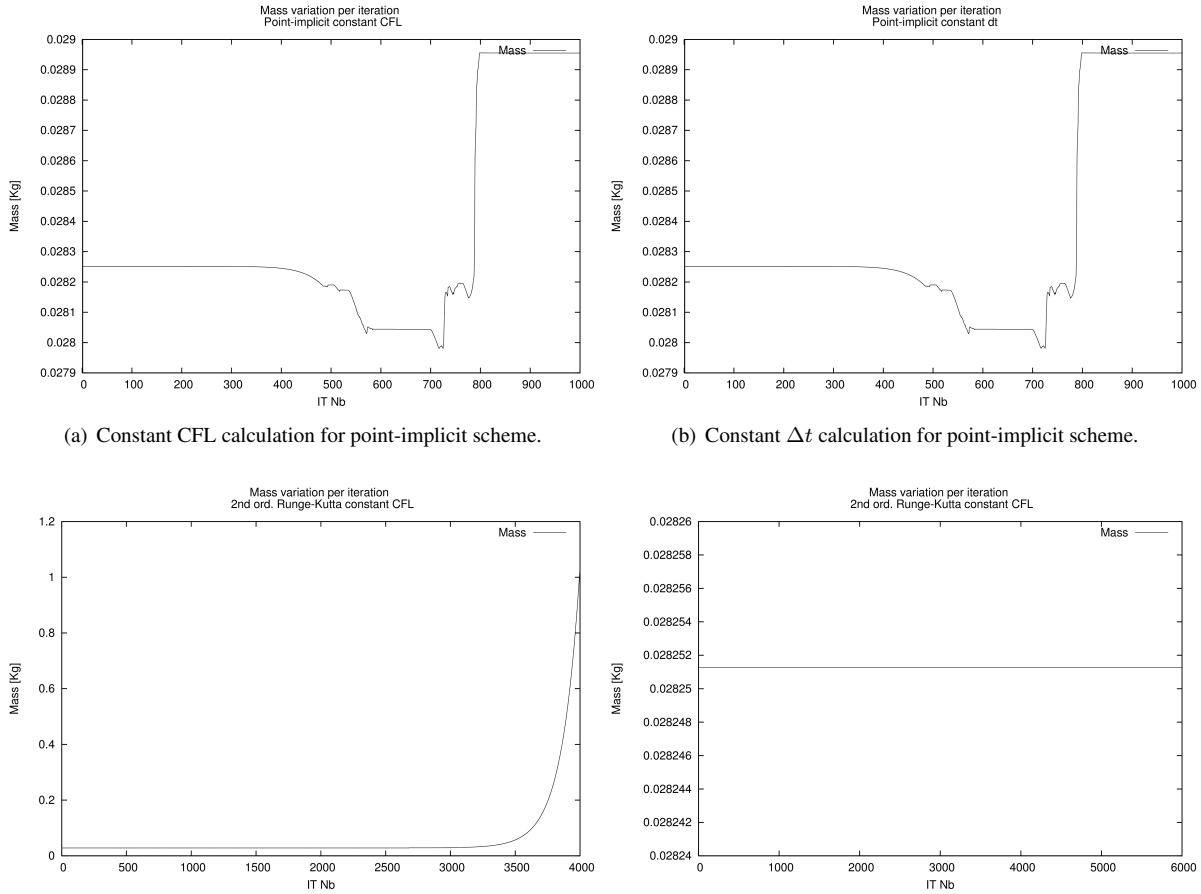

(a) Constant CFL calculation for point-implicit scheme.

(b) Constant Δt calculation for point-implicit scheme.

(c) Constant CFL calculation for explicit RK scheme.

(d) Constant Δt calculation for explicit RK scheme.

Figure 3. Effects of time marching scheme on total mass conservation.

integration schemes by construction. Therefore, for the point implicit integration, the convergence of the sub-iterations has to be achieved in order to obtain a conservative scheme. Furthermore, all the mesh cells have to advance in time using the same Δt value in order to maintain the conservative property of the finite volume method. This is true even for the explicit time marching methods.

6. CONCLUSIONS

A discussion on the issues associated with the coupling of implicit integration methods, for unstructured finite volume formulations, with the spatial discretization based on flux vector splitting schemes is presented in this work. The linearization of inviscid and viscous Jacobians may result in a non-conservative method during the transient phase of the flow simulation, even for the finite volume formulation, which is supposed to be conservative by construction. The present analysis of the numerical formulation and of the computational results obtained has indicated that the time integration can be considered conservative only if the sum of the Jacobian matrices in each column of the linear system matrix is zero and all mesh cells have the same Δt value. Moreover, very popular approximate methods used in many CFD codes, to solve sparse linear systems, such as the point implicit integration, need to achieve convergence of the sub-iterations in order to be conservative during the transient portion of the simulation. This is a very expensive proposition and it can make such approximate solvers as expensive as those which perform the direct solution of the full implicit linear system.

The important conclusion is that care must be exercised in the linearization of time-marching methods for simulations which demand the conservative property. It is important to be aware of the effects of such issue on the physical problem of interest. Physical problems with farfield boundary conditions, very common in simulations for aerospace applications, do

not necessarily need a conservative scheme during the transient portion of a steady state calculation, because the amount of variation in the flow properties, during one time step, is negligible compared to the flux of the same properties that is crossing the open boundaries of the domain. On the other hand, the conservative property is absolutely essential for closed systems, in which the total mass, and other properties, must always be conserved in order to achieve a physical solution. In critical cases, the use of numerical approximations to solve the full implicit linear systems should not be used.

7. ACKNOWLEDGMENTS

The authors would like to acknowledge Conselho Nacional de Desenvolvimento Científico e Tecnológico, CNPq, which partially supported the project under the Research Grants No. 312064/2006-3 and No. 471592/2011-0. Further partial support was provided by Fundação Coordenação de Aperfeiçoamento Passoal de Nível Superior, CAPES, through a Ph.D. scholarship to the first author, and it is also gratefully acknowledged.

8. REFERENCES

Barth, T.J., 1987. "Analysis of implicit local linearization techniques for upwind and TVD algorithms". In *Proceedings of the 25th AIAA Aerospace Sciences Meeting*. AIAA Paper No. 87-0595, Reno, NV.

Harten, A., 1983. "High resolution schemes for hyperbolic conservation laws". *Journal of Computational Physics*, Vol. 49, No. 3, pp. 357 – 393.

Junqueira-Junior, C.A., 2012. *A Study on the Extension of an Upwind Parallel Solver for Turbulent Flow Applications*. Master's thesis, Instituto Tecnológico de Aeronáutica, São José dos Campos, SP, Brasil.

Junqueira-Junior, C.A., Azevedo, J.L.F., Basso, E. and Scalabrin, L.C., 2011. "Study of robust and efficient turbulence closures for aerospace applications". In *32nd Iberian Latin American Congress on Computational Methods in Engineering – CILAMCE XXXII*. Ouro Preto, MG, Brazil.

Lomax, H., Pulliam, T.H. and Zingg, D.W., 2001. *Fundamentals of Computation Fluid Dynamics*. Springer, New York, USA.

MacCormack, R.W. and Candler, G.V., 1989. "The solution of the Navier-Stokes equations using Gauss-Seidel line relaxation". *Computer and Fluids*, Vol. 17, pp. 135–150.

Scalabrin, L.C., 2007. *Numerical Simulation of Weakly Ionized Hypersonic Flow Over Reentry Capsules*. Ph.D. thesis, Department of Aerospace Engineering, The University of Michigan, Michigan, USA.

Steger, J.L. and Warming, R.F., 1981. "Flux vector splitting of the inviscid gasdynamic equations with application to the finite-difference method". *Journal of Computational Physics*, Vol. 40, No. 2, pp. 263–293.

9. RESPONSIBILITY NOTICE

The authors are the only responsible for the printed material included in this paper.